Advanced Healthcare Materials

ADVANCED HEALTHCARE MATERIALS
www.advhealthmat.de

RESEARCH ARTICLE OPEN ACCESS

Stability of Medicinal Nanoemulsions to Spaceflight: Insights From the StarMed Experiment

Modupe Adebowale[1,2,3,4] | Nguyen Van Duc Long[1,2] | Philip M. Williams[4] | Jens Hauslage[6,7,8] | Volker Hessel[1,2,3,5]

[1]School of Chemical Engineering, Adelaide University, Adelaide, Australia | [2]ARC Centre of Excellence Plants For Space, Adelaide University, Adelaide, Australia | [3]Andy Thomas Centre For Space Resources, Adelaide University, Adelaide, Australia | [4]School of Pharmacy, University of Nottingham, Nottingham, UK | [5]School of Engineering, The University of Warwick, Coventry, UK | [6]Institute of Aerospace Medicine, German Aerospace Center, Cologne, Germany | [7]La Trobe Institute For Moelcular Science, La Trobe University, Melbourne, Australia | [8]School of Agriculture, Biomedicine and Enviroment, La Trobe University, Melbourne, Australia

Correspondence: Volker Hessel (volker.hessel@adelaide.edu.au)

Received: 21 April 2026 | **Revised:** 21 July 2026 | **Accepted:** 24 July 2026

Keywords: chitosan-coating | dialysis | melatonin | nanoemulsion | sounding rocket

ABSTRACT

Space missions require liquid drug formulations that remain physically stable and exhibit predictable release under launch, microgravity, and handling stresses. This study examined melatonin-loaded nanoemulsions flown on the MAPHEUS-15 sounding rocket, comparing an uncoated nanoemulsion (MN) with a chitosan-coated nanoemulsion (CCN). Droplet size, polydispersity index (PDI), and zeta potential were measured at Day 0 and after spaceflight, ground vibration testing, matched ground controls, and laboratory storage. Melatonin release was quantified by dynamic dialysis and interpreted using a compartmental mass-transfer model.

Melatonin-loaded nanoemulsion (MN) showed a modest, systematic increase in droplet size under all post-experiment conditions, with unchanged PDI and zeta potential, consistent with time-dependent coalescence and Ostwald ripening rather than a specific microgravity effect. CCN maintained essentially unchanged droplet size, PDI, and zeta potential, indicating interfacial steric stabilization by chitosan. For MN, ageing and sounding-rocket exposure increased the apparent fraction of melatonin available to the aqueous phase, but normalized release profiles overlapped when scaled to the fitted maximum releasable fraction, suggesting unchanged intrinsic release kinetics. In CCN, both the accessible fraction and the release profile were preserved.

Overall, chitosan coating enhanced dimensional and release stability, supporting interfacial polymer coatings as a strategy for robust liquid pharmaceutical formulations for future space medicine.

1 | Introduction

Melatonin is an endogenous hormone with diverse physiological roles, extending well beyond its classical function in circadian rhythm regulation to include musculoskeletal protection. Of particular relevance to spaceflight, melatonin has been reported to mitigate microgravity-induced bone loss by modulating osteoclast activity and preserving bone density [1]. In parallel, its role in sleep regulation and circadian alignment is critical for astronaut performance, as simulated microgravity studies have shown disrupted melatonin secretion and altered sleep physiology [2]. Collectively, these properties position melatonin as a promising therapeutic candidate to support astronaut health during long-duration missions.

One major focus in space pharmacology is understanding how medications behave in microgravity. Because the body's response to drugs can be altered in space, it is essential to characterize how pharmacokinetics and pharmacodynamics may need to be adapted to ensure safe and effective therapy during missions [3–5]. Also, research is examining how space environmental factors, such as ionizing radiation and weightlessness, influence the stability, and performance of pharmaceutical formulations [6, 7]. Space radiation can initiate chemical reactions that accelerate the degradation of active pharmaceutical ingredients, potentially reducing therapeutic effectiveness [8]. At the same time, the absence of gravity may alter the physical characteristics of liquid formulations including nanoemulsions, with implications for their stability and shelf life [9, 10].

Understanding how space-specific factors affect medication stability is therefore crucial for maintaining the safety and efficacy of drug treatments during long-duration missions. In the broader context of human space exploration, it is equally important to investigate how altered gravity influences humans, biological systems, and biochemical processes. Decades of spaceflight research have shown that astronauts and biological model systems, including cells, small animals, and plants, exhibit diverse physiological changes with, skeletal muscle atrophy, bone demineralization, and immune dysregulation among the most consistently reported in astronauts [11–13]. In addition to these systemic effects, biophysical changes such as altered membrane fluidity and modified incorporation of pharmaceutical substances into lipid bilayers have been observed [14]. These findings indicate that gravity shapes both fundamental biophysical properties and complex living systems in ways directly relevant to astronaut health.

The provision of safe and effective drug therapies in space is a critical component of human exploration, particularly as countermeasure to physiological effects of microgravity. Understanding how pharmaceutical formulations tolerate space environment is therefore essential. It is equally important to determine how weightlessness influences advanced drug delivery systems such as nanoemulsions, which offer promising prospects for stable, versatile therapies. These lines of inquiry underpin efforts to safeguard astronaut's health and sustainable human missions to the Moon, Mars, and beyond.

Gravity has been the only constant backdrop against which life has evolved on earth. To investigate how its alteration affects biological and physicochemical systems, several microgravity platforms are used, including sounding rockets, drop towers, parabolic plane flights, satellites, and space stations [15, 16]. Sounding rockets, in particular have contributed substantially to gravitational biology and space medicine by enabling short-duration exposure of cells, small animals, and tissues to real microgravity [17, 18]. For example, in the TEXUS-53 mission, human thyroid cancer cells flown on a sounding rocket showed changes in gene expression related to apoptosis, adhesion, and cytoskeletal organization under microgravity conditions [18]. Such studies are vital for understanding the physiological changes experienced by astronauts during long-duration missions and for developing effective countermeasures against the adverse effects of space travel and altered gravity.

Despite extensive use of sounding rockets and other microgravity platforms to study biological responses to altered gravity, comparatively few investigations have examined the stability and performance of pharmaceutical nanoformulations following real spaceflight exposure. Consequently, experimental evidence describing how liquid drug delivery systems behave under real flight conditions remains limited.

Previous study on the cosmic-ray stability of tablets highlighted the necessity of developing drug formulations tailored to perform reliably in space. In that study, an iron-oxide coating was applied to ibuprofen tablets and was shown to stabilize tablet integrity and reduced active pharmaceutical ingredient (API) degradation under to cosmic rays aboard and outside the International space station (ISS) [19]. Nevertheless, current astronaut medications are designed, licensed, and regulated for use under standard Earth gravity, with largely uncharacterized changes in their efficacy profiles in microgravity. Coatings represent one practical way to modulate and protect drug performance by shielding the active pharmaceutical ingredient from environmental degradation, controlling release kinetics, and enhancing therapeutic effectiveness [20, 21]. However, evidence on the behavior of coated formulations in space, particularly under microgravity, remains scarce. Most studies of coatings and advanced drug delivery systems have been conducted under terrestrial conditions or on simulated microgravity platforms, leaving a gap between laboratory observations and validation under real flight conditions.

This study addresses that gap by investigating the stability and release behavior of chitosan-coated melatonin nanoemulsions following exposure to a MAPHEUS-15 sounding rocket mission. Unlike simulated microgravity platforms, sounding rockets expose formulations to the combined effects of launch vibration, hypergravity, real microgravity and recovery within a single experimental campaign, thereby providing a realistic assessment of pharmaceutical performance under spaceflight condition. Building on prior work on radiation-resistant pharmaceutical formulations and simulated microgravity studies, the present investigation extends those findings through experimental validation in an authentic suborbital environment. Although the physicochemical characterization techniques employed are well established, the novelty of this work lies in applying these methods to pharmaceutical nanoemulsions recovered from real spaceflight and directly comparing coated and uncoated formulations under flight condition. These findings contribute experimental evidence supporting the development of robust liquid medicines for future orbital and deep-space missions.

2 | Methodology

2.1 | Experimental Workflow and Study Timeline

This study investigated the stability of melatonin-loaded nanoemulsions under spaceflight conditions utilizing the MAPHEUS-15 sounding rocket platform. The experimental workflow progressed through distinct phases: formulation and initial characterization in Adelaide, Australia; payload integration at the German Aerospace Center (DLR); spaceflight operations at ESRANGE Space Center in Kiruna, Sweden; and post-flight analysis in Adelaide (Figure 1).

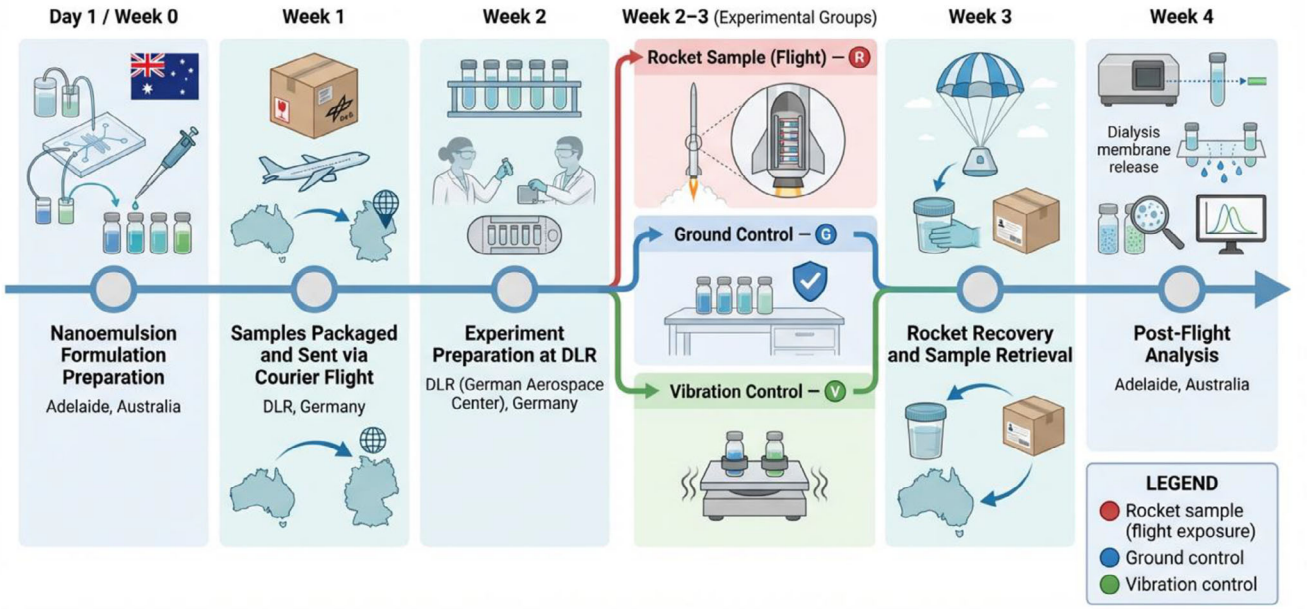

FIGURE 1 | Timeline of the StarMed MAPHEUS-15 sounding rocket nanoemulsion experiment.

2.2 | Sample Preparation and Transport

Melatonin-loaded nanoemulsions (NEs) and chitosan-coated nanoemulsions were prepared at the Adelaide University using a spontaneous low-energy emulsification approach, as previously described [22], with minor adaptations for the present study. Melatonin was dissolved in medium-chain triglyceride (MCT) oil to form the oil phase (3 mg mL^{-1}). A surfactant mixture consisting of Tween 80 and Span 80 (63:37 wt%), together with glycerol as a co-solvent (2:1 ratio), was used to stabilize the emulsion system. The surfactant mixture and melatonin-loaded oil were combined at a surfactant-to-oil ratio of 1.0, yielding a homogeneous oil phase under controlled stirring and temperature conditions. Nanoemulsions were generated using a microfluidic droplet formation system equipped with dual HPLC pumps and a T-mixer (0.5 mm internal diameter). The oil phase and aqueous phase (10 mM phosphate buffer or 0.1% chitosan solution) were injected at defined flow rates to produce droplets that subsequently passed through a coiled flow inverter, enhancing mixing and residence time within the microchannel. The resulting formulations were dispensed into high-performance liquid chromatography (HPLC) 2 mL glass vials, sealed and labelled as uncoated melatonin nanoemulsion (MN) and/or chitosan coated melatonin nanoemulsion (CCN). Four replicate vials were prepared for each experimental condition, with one vial reserved as a backup in case of damage during transit. Three independent samples were analyzed.

2.3 | Payload Integration

Upon arrival at the German Aerospace Center (Deutsches Zentrum für Luft- und Raumfahrt, DLR), Germany, the nanoemulsion vials were integrated into the NyMEX experimental module using custom 3D-printed holders designed to secure HPLC vials during flight operations (Figure 2). The holders were mounted with Velcro tape in two dimensions within a vacuum-tight experimental chamber to protect samples from pressure variations during ascent and descent phases under ambient temperatures (22°C ± 2°C).

Samples were then allocated to four experimental groups with four vials of each nanoemulsion formulation assigned per condition:

I. Ground laboratory control (Ground Lab): Samples remained in Adelaide for the duration of the study and served as a storage/time control to assess changes arising from laboratory storage alone.

II. Ground flight control (Ground): Samples were transported from Adelaide to the German Aerospace Center (DLR), Germany, together with the flight payload, remained on the ground throughout the campaign, and were subsequently transported back to Adelaide without exposure to vibration testing or sounding rocket flight. This group controlled for transport, storage and handling associated with the campaign.

III. Vibration control (Vibration): Samples accompanied the flight payload between Adelaide and Germany and were subjected only to the standard pre-flight vibration qualification test before being returned to Adelaide.

IV. Flight: Samples accompanied the payload throughout the campaign and were launched aboard the MAPHEUS-15 sounding rocket, experiencing launch vibration, hypergravity, microgravity and recovery before return to Adelaide for analysis.

With the exception of the Ground Lab Control, the Ground, Vibration and Flight samples all followed the same international transport pathway between Adelaide and Germany, after which they underwent their respective experimental exposures.

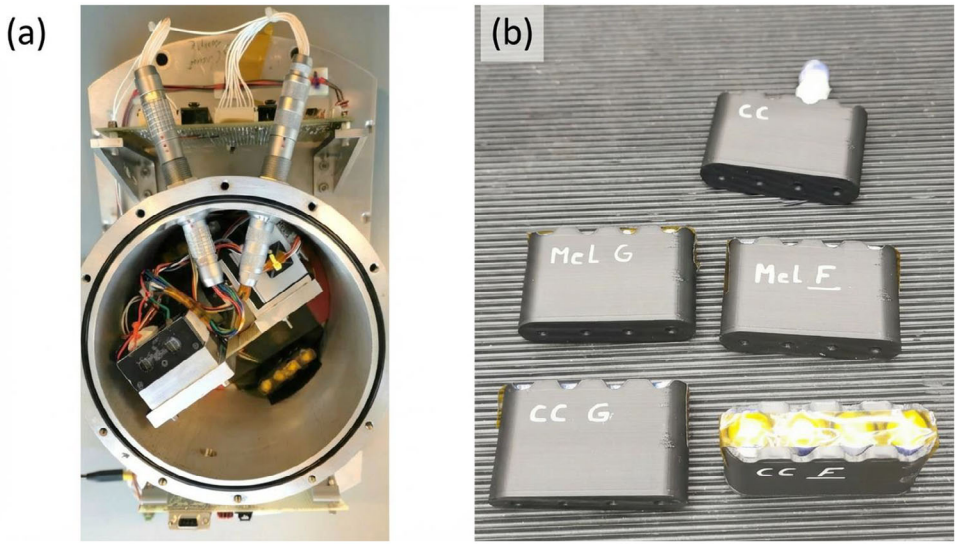

FIGURE 2 | Experimental hardware used for the MAPHEUS-15 nanoemulsion spaceflight experiment. (a) NyMEx late access unit with open vacuum tight vessel. The samples are located in the upper left part inside the vessel. The four, white caps of the glass vials are visible. The samples were attached with Velcro tape in two dimensions, bottom and side. In this accommodation the vibration test and flight experiment were performed. (b) Custom 3D-printed sample holders used to secure the nanoemulsion HPLC vials.

2.4 | MAPHEUS-15 Sounding Rocket Mission

The MAPHEUS (Materialphysikalische Experimente unter Schwerelosigkeit) sounding rocket programme, operated by the DLR Institute for Materials Physics in Space, provides a well-characterised and reliable platform for short-duration microgravity research. The MAPHEUS-15 rocket was launched on 11 November 2024 at 08:38 Central European Time (CET) from the Skylark launch tower at the ESRANGE Space Center, Kiruna, northern Sweden.

The rocket reached an apogee of approximately 309–310 km on a suborbital ballistic trajectory. The powered ascent phase lasted about 51 s, during which the payload experienced a peak acceleration of 11.8 g. Following motor burnout and separation, the payload entered a microgravity phase of 441 s with gravitational acceleration reduced to sub-milli-*g* levels, providing a high-quality microgravity environment. After re-entry and landing, the payload was recovered and the samples remained sealed within the NyMEX experimental chamber until return to Adelaide for analysis.

2.5 | Vibration Testing Protocol

Environmental qualification vibration testing was performed on the fully integrated payload prior to launch, in accordance with standard sounding rocket acceptance procedures. Vibration control samples were exposed to random vibration inputs of 7.5 g root mean square (RMS) in both the lateral X and Y axes, and 10.0 g RMS in the longitudinal Z axis (axial direction). These test parameters were selected to envelope the expected launch vibration environment and to verify structural integrity of the payload and its experimental contents.

2.6 | Post-flight Analysis

Following payload recovery, all samples were returned to Adelaide, Australia, for post-flight analyses. Physicochemical characterisation was performed by measuring droplet size, PDI, and zeta potential, using dynamic light scattering (DLS). In addition, in vitro dialysis-based drug release studies were conducted to assess whether spaceflight or vibration exposure had altered the release kinetics of melatonin from the nanoemulsion matrix.

Comparative analysis across the Day 0 reference and four post-preparation groups (ground laboratory control, ground flight control, vibration control, and flight), enabled the individual contributions of storage, international transport, vibration and spaceflight to be distinguished. This systematic approach allowed any observed changes to be attributed to specific physical stressors, providing mechanistic insight into nanoemulsion behaviour under conditions relevant to future long-duration spaceflight missions.

2.7 | In Vitro Melatonin Release Study

The in vitro melatonin release study was performed as previously described [22] using the dialysis bag diffusion method. This approach was employed as a comparative tool to evaluate whether exposure to launch, vibration, microgravity and storage time altered the release behavior of the drug formulation under standardized conditions.

Flight, vibration and ground samples, together with the Day 0 ground control and the 4-week stored ground control, were evaluated in phosphate-buffered saline (PBS, pH 7.4). Dialysis membranes (molecular weight cut-off: 12–14 kDa) were pre-soaked in Milli-Q water for 12 h prior to use. Subsequently, 1.8 mL of each formulation was transferred into separate dialysis bags

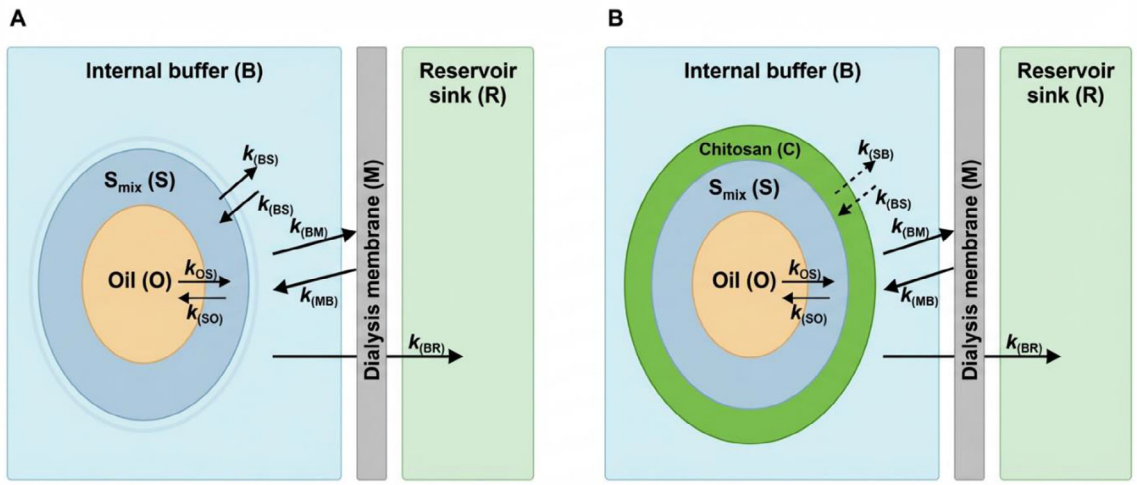

FIGURE 3 | Schematic representation of drug release mechanisms from nanoemulsion systems. (A) Uncoated system: showing drug partitioning and transport from the oil phase (O) through the surfactant mixture (Smix, S) into the internal buffer (B), followed by diffusion across the dialysis membrane (M) into the reservoir sink (R). (B) Coated system: have additional polymeric barrier surrounding the Smix *layer, modulating drug diffusion from the oil phase (O/S) to the internal buffer (B) The coating introduces an additional resistance to mass transfer, altering the effective rate constants between compartments.*

($n = 3$), which were securely sealed and immersed in 50 mL of release medium. The dialysis bags were incubated at 37°C ± 2°C with continuous shaking at 150 rpm.

At predetermined time intervals, 1 mL aliquots were withdrawn from the release medium and immediately replaced with an equal volume of fresh pre-warmed PBS to maintain sink conditions and a constant release volume. Melatonin concentration in the collected samples was quantified by UV spectrophotometry at 278 nm, and the cumulative percentage of melatonin released was calculated.

2.8 | Statistical Analysis and Mathematical Modelling

For each experimental group, three independent samples ($n = 3$) were analyzed. Each sample was measured in triplicate (three technical measurements), and the mean value was used for statistical analysis. Results are presented as mean ± standard deviation (SD). Statistical analyses and multiple comparisons were performed using GraphPad Prism (version 10.0; GraphPad Software, San Diego, CA, USA). Comparisons among experimental groups were conducted using one-way analysis of variance (ANOVA) with Brown–Forsythe/Welch correction, followed by Dunnett's multiple comparisons test using Day 0 as the reference. A p-value < 0.05 was considered statistically significant.

The experimentally measured cumulative melatonin release data obtained from the dialysis experiments were interpreted using a compartmental diffusion model that accounted for both drug release from the nanoemulsion and subsequent diffusion across the dialysis membrane. The model comprised five interconnected compartments representing the oil phase (O), surfactant phase (S), internal aqueous buffer (B), dialysis membrane (M), and external reservoir sink (R) compartments as illustrated in Figure 3. Drug transport between compartments was assumed to follow first-order kinetics governed by the corresponding transfer rate constants, k_{xy}. The temporal evolution of drug concentration in each compartment was described by a system of ordinary differential equations of the form:

$$\frac{\mathrm{d}[D_O]}{\mathrm{d}t} = -k_{OS}[D_O] + k_{SO}[D_S]\frac{V_S}{V_O}$$

$$\frac{\mathrm{d}[D_S]}{\mathrm{d}t} = -(k_{SB} + k_{SO})[D_S] + k_{OS}[D_O]\frac{V_O}{V_S} + k_{BS}[D_B]\frac{V_B}{V_S}$$

$$\frac{\mathrm{d}[D_B]}{\mathrm{d}t} = -(k_{BR} + k_{BS} + k_{BM})[D_B] + k_{SB}[D_S]\frac{V_S}{V_B} + k_{MB}[D_M]\frac{V_M}{V_B}$$

$$\frac{\mathrm{d}[D_R]}{\mathrm{d}t} = k_{BR}\ [D_B]\frac{V_B}{V_R}$$

where $[D_x]$ is the concentration of drug in compartment x of volume V_x, and k_{xy} is the rate constant for the transfer from compartment x to compartment y of O, S, B, M, and R.

Model parameters corresponding to known experimental quantities were fixed, and the remaining transport rate constants were estimated by fitting the model to the experimental release profiles. Model optimisation was performed using custom-written software implementing a simulated-annealing simplex algorithm based on Numerical Recipes in C: The Art of Scientific Computing [46]. Model uncertainty was assessed by bootstrap resampling; shaded regions in the release curve represent the resulting 95% confidence intervals. Data symbols show experimentally measured cumulative release values (mean ± SD, $n = 3$), and solid curves represent the fitted compartmental diffusion model.

TABLE 1 | Summary of results for droplet sizes, polydispersity index and zeta potential. MN = melatonin nanoemulsion; CCN = chitosan coated melatonin nanoemulsion, for each parameter. Three independent samples (n = 3) were analysed for each experimental group and each sample was measured in triplicate.

Batch	Droplet size (d.nm)	PDI	Zeta potential (mV)
MN day 0	162 ± 1.1	0.132 ± 0.02	−10.8 ± 1.0
MN flight	176 ± 1.5	0.146 ± 0.02	−12.9 ± 0.9
MN ground	176 ± 1.6	0.149 ± 0.02	−11.8 ± 0.5
MN vibration	176 ± 1.6	0.148 ± 0.02	−11.3 ± 0.7
MN ground lab	167 ± 1.5	0.125 ± 0.01	−10.5 ± 1.7
CCN day 0	149 ± 1.2	0.166 ± 0.01	−6.5 ± 0.7
CCN flight	150 ± 1.3	0.164 ± 0.02	−8.1 ± 0.8
CCN ground	151 ± 1.2	0.173 ± 0.02	−7.2 ± 0.5
CCN vibration	150 ± 1.3	0.174 ± 0.01	−7.9 ± 0.6
CCN ground lab	151 ± 1.3	0.174 ± 0.01	−6.6 ± 0.6

3 | Results and Discussion

3.1 | Index and Zeta Potential

For nanoemulsions intended as drug carriers in spaceflight, optimizing any interfacial coating is only meaningful if the underlying dispersed system remains physically and colloidally stable under mission-relevant stresses. Changes in mean droplet size and size distribution directly modulate diffusion path length and interfacial area, thereby influencing drug transport across the coating and altering the effective release capacity of individual droplets. This coupling between droplet dimensions and release performance has been repeatedly highlighted for lipid nanoemulsions and polymer-coated carriers, where smaller droplets and lower polydispersity increase interfacial area and thereby enhance dissolution, bioavailability, and modulate release kinetics [23–25].

Microgravity- or vibration-induced shifts in these static properties could therefore propagate into altered macroscopic release behavior, even when the chemical composition remains unchanged. In parallel, zeta potential is a key descriptor of colloidal stability under the Derjaguin–Landau–Verwey–Overbeek (DLVO) framework, which balances van der Waals attraction against electrostatic double-layer repulsion and predicts the propensity of nanoemulsions to aggregate, flocculate or coalesce [26]. Alterations in surface charge under spaceflight conditions could modify the energy barrier to droplet–droplet approach and introduce a dynamic instability component that feeds back into drug release.

3.1.1 | Droplet Sizes

The MN formulation was susceptible to time-dependent droplet growth across all conditions. Relative to the Day 0 reference (162 ± 1.1 nm), mean droplet sizes increased to 176 ± 1.6 nm in the flight, ground and vibration batches, and to 167 ± 1.5 nm in the ground laboratory control (Table 1, Figure 4). This consistent increase across all post-experiment samples indicates that droplet growth reflects general ageing and handling rather than a microgravity-specific effect. Such behavior is compatible with reports that nanoemulsion stabilized solely by low-molecule-weight surfactants can undergo gradual size increase driven predominantly by Ostwald ripening, which in turn can facilitate subsequent coalescence. In this mechanism, Laplace pressure difference between droplets of different size, promoting molecular diffusion of dispersed oil from smaller to larger droplets over time [27].

The absence of any additional size increase in the flight samples compared with the ground and vibration groups suggests that, over the short microgravity window of a sounding-rocket mission, gravity-related hydrodynamic effects do not outweigh intrinsic ripening processes in the uncoated formulation. However, the CCN maintained droplet sizes statistically indistinguishable from Day 0 (149 ± 1.2 nm) under all conditions, with values of 150 ± 1.3 nm (flight and vibration) and 151 ±1.3 nm (ground and ground laboratory control). This invariance strongly supports a stabilizing role for the chitosan shell, which provides both steric hindrance and reinforces the interfacial layer in line with previous reports on polysaccharide- and chitosan-coated nanoemulsions [28, 29]. The hydrated polymer layer increases effective droplet separation and introduces a diffusion barrier to molecular exchange, thereby attenuating both coalescence and Ostwald ripening [28–30]. The fact that droplet size remained stable even after exposure to launch vibration indicates that the chitosan network withstands substantial mechanical input without interfacial failure. Overall, these findings demonstrate that chitosan coating transforms the MN system from an ageing-sensitive nanoemulsion into a dimensionally robust carrier suitable for microgravity studies and, by extension, for longer-duration space missions where cumulative destabilization risks are greater.

3.1.2 | Polydispersity Index

Despite the divergent behavior in mean droplet size, PDI values for both MN and CCN remained low and statistically unchanged

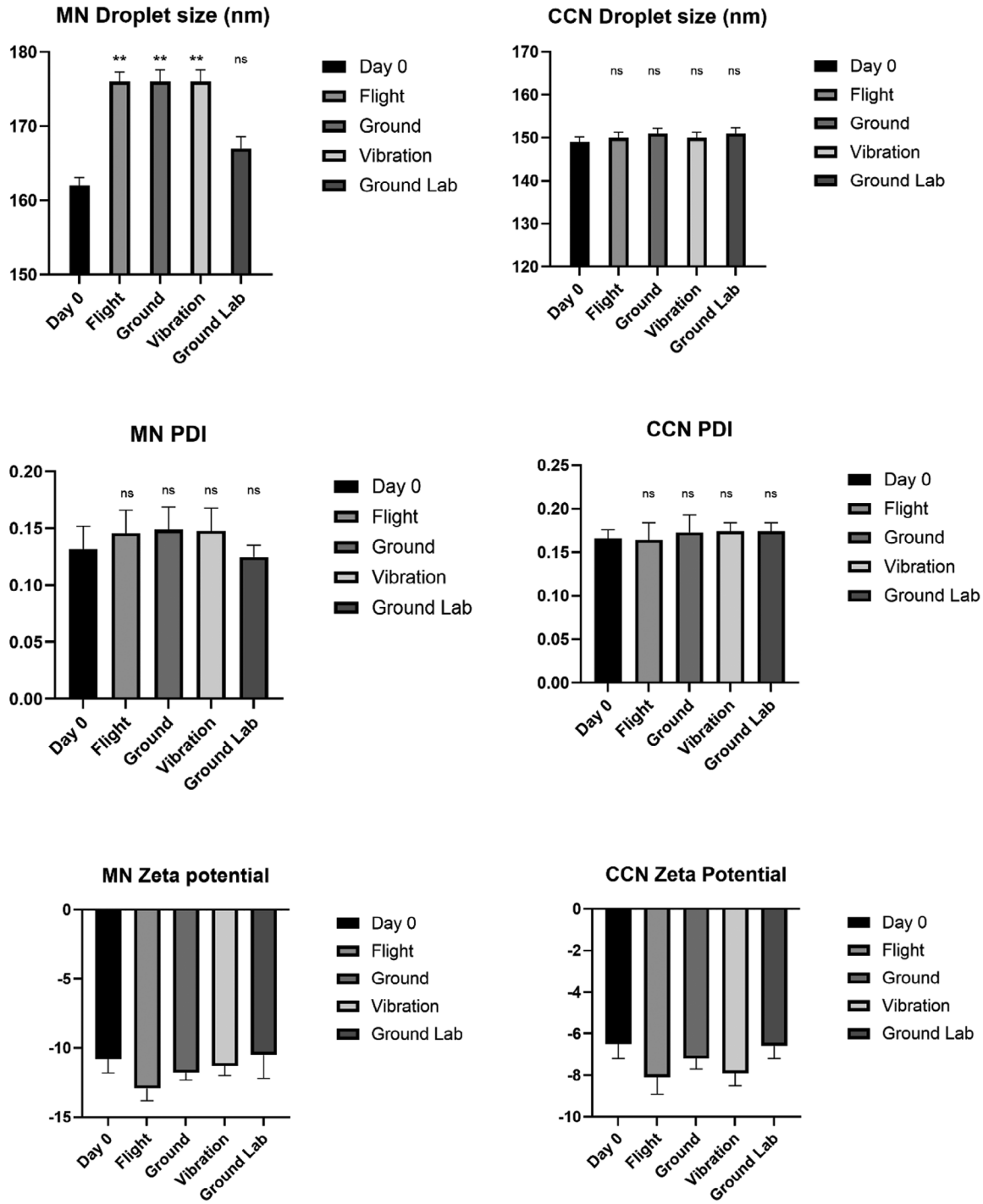

FIGURE 4 | Effect of sounding rocket flight, vibration and ground controls on droplet size, polydispersity index (PDI) and zeta potential of MN and CCN at Day 0 and post-experiment. Data are mean ± SD (n = 3). Statistical analysis was performed in GraphPad Prism using one-way ANOVA with Brown–Forsythe/Welch correction followed by Dunnett's multiple comparisons test versus Day 0. For MN, droplet size was significantly increased in Flight, Ground and Vibration samples (**$p < 0.01$) while PDI and zeta potential showed no significant changes.

relative to Day 0 across all experimental conditions. For MN, PDI ranged from 0.125 ± 0.02 (ground Lab) to 0.149 ± 0.02 (ground), compared with 0.132 ± 0.02 at Day 0. For CCN, PDI values were confined to 0.164 ± 0.02 to 0.174 ± 0.01, relative to 0.166 ± 0.01 at Day 0. All values lie within the range typically associated with monodisperse or narrowly polydisperse nanoemulsions, indicating that the droplet populations remained relatively uniform even when the MN droplets grew in size.

This pattern suggests that the dominant destabilization pathway in MN was a near-uniform shift toward slightly larger droplets, rather than the development of a broad, multimodal size distribution that would indicate catastrophic coalescence or extensive flocculation. For CCN, the combination of stable mean size and low, unchanged PDI further supports that the chitosan coating suppresses heterogeneity-generating events under both microgravity and terrestrial conditions. From a drug-delivery

standpoint, preservation of a low PDI is advantageous because it maintains a predictable interfacial area and diffusion geometry across the droplet population, favoring reproducible release kinetics [31].

3.1.3 | Zeta Potential

Zeta potential measurements provided complementary insight into the electrostatic aspect of nanoemulsion stability. In the MN system, zeta potential remained moderately negative and statistically stable across all conditions, with values of −12.9 ± 0.9 mV (flight), −11.8 ± 0.5 mV (ground), −11.3 ± 0.7 mV (vibration) and −10.5 ± 1.7 mV (ground lab), compared with −10.8 ± 1.0 mV at Day 0. These data suggest that neither microgravity nor vibration measurably altered the electrostatic environment at the bare surfactant interface over the experimental timescale. Although MN exhibited significant droplet size growth, the broadly unchanged zeta potential indicates that destabilization is more likely associated with progressive drug solubilization into surfactant micelles, facilitated by the excess Tween and Span present well above their critical micelle concentration (CMC), than with loss of electrostatic repulsion at the droplet interface. Because hydrodynamic diameters were obtained from intensity-weighted DLS measurements, any emerging population of small micelles would contribute only weakly to the scattering signal and cannot be quantified directly.

For the CCN, zeta potential values were slightly less negative at Day 0 (−6.5 ± 0.7 mV) and remained within a narrow band across all conditions: −8.1 ± 0.8 mV (flight), −7.2 ± 0.5 mV (ground), −7.9 ± 0.6 mV (vibration), and −6.6 ± 0.6 mV (ground lab). Post-experiment samples therefore showed a modest tendency toward more negative zeta potentials relative to the Day 0, with the largest shift in the flight and vibration batches. Given the overlapping standard deviations and the limited sample size (n = 3), these changes are best interpreted as minor fluctuations around a stable mean, rather than evidence for systematic gain or loss of surface charge. Importantly, this slight increase in negative charge did not translate into measurable changes in droplet size or PDI, indicating that the electrostatic landscape of the CCN interface remained within a regime that, together with steric protection from the chitosan layer, was sufficient to prevent aggregation or coalescence.

Mechanistically, the small drift toward more negative values after storage and flight may reflect subtle changes in ion adsorption at the chitosan-modified interface, pH-dependent protonation equilibria of chitosan amino groups, or slow rearrangement of polymer chains at the oil–water boundary [32]. However, the absence of associated growth in droplet size or broadening of PDI suggests that these interfacial adjustments did not compromise colloidal integrity. These observations highlight a key advantage of polymer-coated nanoemulsions: steric contributions to interfacial stabilization can buffer modest variations in zeta potential, partially decoupling physical stability from the absolute magnitude of surface charge.

The present flight campaign primarily assessed post-flight colloidal stability through droplet size, PDI and zeta potential. The limited quantity of formulation for sounding rocket mission necessitated prioritization of physicochemical measurements and drug-release analyses, and pre- versus post-flight Cryo-TEM or extended stability testing were therefore not included within the scope of the present study. Baseline Cryo-TEM characterization and terrestrial stability evaluation of these formulations have been reported previously [22], establishing morphology and stability prior to flight. Future missions with larger recoverable sample volumes could incorporate complementary structural analyses and extended post-flight stability studies to further probe potential nanoemulsion structural changes associated with spaceflight exposure.

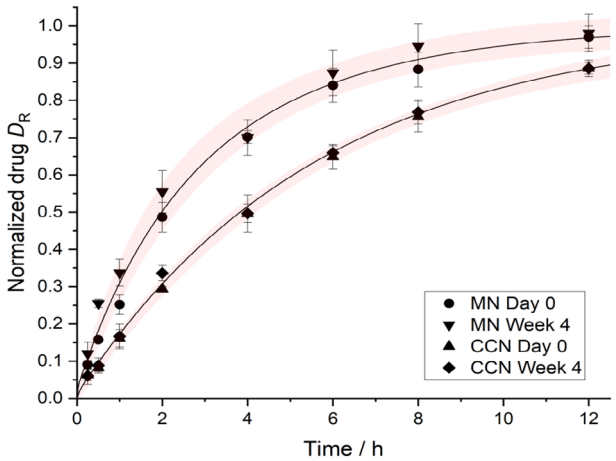

FIGURE 5 | Time-dependent normalized drug release profiles from MN and CCN formulations at Day 0 and after 4 weeks of storage. Symbols represent experimentally measured cumulative melatonin release (mean ± SD, n = 3). Solid lines represent the fitted compartmental diffusion model, while the shaded regions denote the corresponding 95% confidence intervals estimated by bootstrap analysis.

3.2 | Drug Release Profiles of Melatonin Nanoemulsions (Time/Storage Dependent Effect)

The experimentally measured cumulative melatonin release profiles of the uncoated (MN) and chitosan-coated (CCN) nanoemulsions are shown in Figure 5. Experimental data are plotted as symbols (mean ± SD, n = 3), and the solid curves represent the fitted compartmental diffusion model. Because the dialysis setup captures both drug release from the formulation and diffusion across the dialysis membrane, the compartmental model was used to disentangle changes in drug partitioning from changes in intrinsic release kinetics. In the uncoated system, rapid bidirectional exchange between oil and surfactant (large k_{OS}, k_{SO}) causes these compartments to behave effectively as a single droplet-associated reservoir. Exchange between the droplet reservoir and the internal aqueous buffer is governed by k_{SB} and k_{BS}, while subsequent adsorption to dialysis membrane and diffusion into the reservoir sink and described by k_{BM}, k_{MB}, and k_{BR} (parameters obtained by measuring the passage of drug from buffer to the reservoir across the dialysis membrane; Figure S1). Between Day 0 and week 4, storage allows a larger fraction of melatonin to equilibrate out of the droplet interior (O/S) into the aqueous buffer (B), consistent with its higher effective solubility in the surfactant-rich compartment than in the neat oil.

In the model, the Day 0 experiment assumes initial equilibration between oil and surfactant only, whereas the week 4 experiment assumes initial equilibration between oil, surfactant and buffer. Importantly, the same set of rate constants k_{xy} adequately described both datasets. Thus, storage did not substantially alter the intrinsic release kinetics; instead, the higher plateau at week 4 reflects an increased fraction of drug already accessible to, or readily exchangeable with, the aqueous phase at $t = 0$, rather than a time-dependent change in diffusion behavior. The increased release is plausibly explained by partial solubilization of melatonin within surfactant micelles formed during storage, given that both surfactants were present well above their critical micelle concentrations.

In the coated system, the chitosan introduces an additional diffusional barrier around the droplet, retarding exchange between S and B. In the model, the coated data are captured by scaling both k_{SB} and k_{BS} of the uncoated case by a common factor (~0.1), thereby slowing drug movement out of and back into the droplets while preserving the equilibrium partition (solubilities) between surfactant and buffer. The close similarities between the week 0 and week 4 release profiles, combined with the unchanged droplet size data, indicates that chitosan effectively stabilized the droplets over the storage period. Overall, the release data and compartmental fits distinguish two behaviors: an uncoated nanoemulsion in which ageing drives additional drug into aqueous and peripheral compartments (including micelles), increasing the apparent extent of release; and a chitosan-coated nanoemulsion, in which slowed droplet–buffer exchange maintains both the interfacial barrier function and storage-robust release performance.

Analysis of the StarMed sounding rocket experimental groups using the same compartmental model showed that time and handling stresses primarily influenced the accessible fraction of melatonin in the uncoated nanoemulsions, without altering their intrinsic release kinetics. For MN samples, flight-exposed samples displayed higher apparent cumulative release than their matched ground controls; however, when normalized to the fitted total releasable amount, the release curves remained closely superimposable (Figures S2–S7). This indicates that the underlying release kinetics of MN were not measurably changed across the ground, flight and vibration conditions, despite differences in the apparent accessible fraction of drug at $t = 0$. In the coated formulations, the release pattern remained consistent with the presence of a chitosan barrier that retards diffusion between the internal droplets and the surrounding buffer while stabilizing droplet size. The CCN groups maintained both their fitted accessible fraction and normalized release profiles across the conditions. These data could be described using the same scaled k_{SB} and k_{BS} values as in the terrestrial storage study, implying that the polymer shell continues to suppress droplet–buffer exchange and mitigate changes in drug partitioning associated with the cumulative flight and handling stresses. These findings suggest that, for uncoated nanoemulsions, the combination of handling stress and ageing over time may increase early in vivo drug availability, whereas interfacial chitosan coatings confer tolerance by preserving both release kinetics and accessible fraction under the investigated spaceflight and control conditions.

3.3 | Comparison with Previous Microgravity Studies and Study Limitations

The present findings align with earlier work examining nanoemulsion and emulsion stability under simulated microgravity. In our previous study, Adebowale et al. [22], the same melatonin-loaded uncoated and chitosan-coated nanoemulsion systems maintained their principal physicochemical characteristics over 28 days of random positioning machine (RPM) gravity-vector averaging, with the chitosan-coated formulation showing greater resistance to destabilization. Dantuma et al. [9] likewise investigated drug-loaded nanoemulsions, including a melatonin formulation, under simulated microgravity using a three-dimensional clinostat and reported overall physicochemical stability during the exposure. These studies indicate that nanoemulsion systems can retain colloidal stability under different ground-based altered-gravity simulations.

However, interpretation of ground-based microgravity data requires consideration of platform-specific artefacts. Schmidt et al. [47] demonstrated that RPM operating conditions can induce fluid motion within multiphase systems, potentially influencing droplet behavior independently of gravity-vector averaging. Thus, while RPM and clinostat platforms enable longer-duration, controlled experiments, they do not fully reproduce the conditions encountered during actual spaceflight. The present sounding rocket study extends these observations into a real suborbital environment, combining brief real microgravity with launch vibration, hypergravity, re-entry, and recovery. Despite substantial differences in platform, exposure duration and mechanical stresses, the consistent physicochemical stability of the chitosan-coated formulation across simulated and real flight environments supports the protective role of the polymeric interfacial coating. Overall, these studies demonstrate the complementary value of ground-based microgravity analogues and real-flight platforms.

The significance of the present work therefore extends beyond the physicochemical measurement themselves. Metrics such as droplet size, PDI, zeta potential and release kinetics are well-established for nanoemulsion characterization, but their application to pharmaceutical formulations recovered after real spaceflight remains limited. By bridging ground-based simulated microgravity data with a suborbital sounding-rocket mission, this study provides additional evidence that chitosan-coated nanoemulsions can retain their physicochemical and drug-release characteristics following spaceflight-associated stresses.

At the same time, several limitations must be acknowledged. The present study evaluates the cumulative effects of the complete sounding rocket flight profile rather than isolating the specific role of microgravity. Although a dedicated vibration control was included to help disentangle launch-related mechanical stresses, the formulations experienced a sequence of conditions comprising launch vibration, hypergravity, brief microgravity, re-entry, recovery and restoration to earth gravity before post-flight characterization. In situ physicochemical measurements during the microgravity phase were not feasible, and the individual

contributions of each flight phase cannot be fully separated on the basis of post-flight data only.

It should also be recognized that microgravity-specific effects may be transient or reversible. The absence of gravity-driven sedimentation and buoyancy-driven convection could, in principle, influence droplet interactions, interfacial organization, molecular transport and drug partitioning within nanoemulsions during microgravity exposure. Such changes, if present, may diminish or reverse during re-entry and subsequent return to Earth gravity and therefore may not be detectable by end-point post-flight analysis. Accordingly, the present findings are best interpreted as evidence of formulation resilience to the cumulative suborbital flight environment, rather than as a definitive assessment of isolated microgravity effects.

Future investigations using long-duration orbital platforms, ideally incorporating in situ or real-time analytical capabilities, will be required to distinguish transient microgravity-induced changes from those associated with other phases of spaceflight and to determine whether microgravity-specific effects are reversible or persist under sustained exposure.

4 | Conclusions

This study provides one of the first experimental evaluations of pharmaceutical nanoemulsions recovered from a sounding rocket mission, helping to bridge the gap between conventional laboratory work, simulated microgravity investigations and authentic suborbital spaceflight. Using established physicochemical characterization methods together with mechanism-based release modelling, we show that chitosan-coated melatonin nanoemulsions can retain their structural integrity and controlled-release behavior after exposure to launch vibration, hypergravity, microgravity, and recovery. The uncoated MN formulations exhibited a small but consistent increase in droplet size across all post-experiment groups compared with Day 0, while maintaining low, unchanged PDI and stable zeta potential. These observations are consistent with general ageing and Ostwald ripening rather than a microgravity-specific instability. Four-week storage and spaceflight exposure increased the apparent melatonin release plateau from MN; however, normalized release profiles and fitted rate constants indicated that intrinsic release kinetics were largely unchanged. The differences are therefore attributed to pre-equilibration and drug redistribution, likely into micellar phases formed during storage.

In contrast, the chitosan-coated nanoemulsion maintained droplet size, polydispersity, and zeta potential within experimental variability across storage, vibration, and flight. Its release behavior remained well described by a model in which surfactant–buffer exchange is uniformly slowed while the overall partitioning pattern is preserved. Under the weeks-scale storage and single short-duration microgravity exposure tested, the chitosan coating acted as a stabilizing interfacial barrier that limited droplet growth and maintained both the accessible drug fraction and the release profile.

Although these experiments do not establish long-term in-flight performance, they support the view that relatively simple polymer coatings can substantially enhance the structural and kinetic robustness of nanoemulsion formulations, identifying chitosan-stabilized nanoemulsions as a promising platform for extended-duration space pharmacy applications. Overall, this work demonstrates that chitosan-coated nanoemulsions possess excellent resilience to the combined mechanical and gravitational stresses encountered during suborbital flight, providing experimental evidence to support the development of robust liquid pharmaceutical formulations for future lunar, orbital and deep-space missions.

5 | Outlook

Spaceflight experiments often address fundamental questions, such as how microgravity influences organized soft matter, including nanoemulsions. Their transient nature, limited data and interpretive challenges, further complicated by transport and handling stresses, can nonetheless constrain definitive conclusions.

The StarMed study provides a robust ‘negative proof’ regarding microgravity impact within the tested regime: neither the uncoated MN nor the chitosan-coated CCN exhibited microgravity-driven changes in droplet size, PDI, zeta potential, or release kinetics beyond time-dependent ageing. MN showed modest droplet growth and an increased accessible drug fraction after storage and flight, attributable to Ostwald ripening and surfactant-mediated partitioning rather than gravitational effects, whereas CCN preserved all physicochemical metrics across conditions, confirming chitosan’s steric stabilization capacity under launch vibrations (~7.5 to 10 g RMS), approximately 6 to 7 min of microgravity, and re-entry forces.

Paradoxically, this robustness underscores the need for more stringent scrutiny of positive microgravity signals in future work. Spaceflight data risk conflating weak gravitational effects with aleatory (statistical) noise or epistemic uncertainties from incomplete models, imperfect ground truth, sampling bias, single-event upsets induced by cosmic rays [33], radiation-thermal swings [34], or communication dropouts [35]. Pre-flight logisticss further amplify this risk: road and air transport impose continuous vibrations (~0.04 to 0.20 g) and discrte shocks reaching 4 to 6 g [36, 37] followed by rocket ascent loads of several g (3 to 4 g, e.g., Falcon 9 at ~3.2 to 4.1 g [38, 39]) and broadband mechanical excitation across a wide frequency range, (5 to 200 Hz) [40]; typically characterized via RMS and PSD metrics [41]. Against this backdrop, subtle microgravity signatures can be obscured or mimicked by non-gravitational perturbations.

Building on Australia’s first NASA ISS-led cosmic-ray tablet study [19] and the emerging sounding-rocket data, there is a clear need for enhanced experimental designs capable of detecting small microgravity effects in soft-matter and pharmaceutical systems. Signal amplification through higher-sensitivity formulations and measurement strategies is required to rise above aleatory noise, while epistemic errors must be reduced through standardized vibration profiles [41], well-characterized transport histories and harmonized analysis pipelines. Where datasets remain small or noisy, as is often intrinsic to space [42], artificial intelligence offers promising tools: anomaly detection to identify biases and aliasing,

proxy datasets derived from clinostats and RPM experiments [43], synthetic data for augmentation [44], and machine-learning approaches tailored for small-n space data and transfer learning in space medicine [45].

Author Contributions

Nguyen Van Duc Long: formal analysis, supervision, Writing – review and editing, validation, investigation. **Volker Hessel:** conceptualization, methodology, validation, formal analysis, supervision, project administration, writing – review and editing, investigation. **Modupe Adebowale:** conceptualization, methodology, data curation, investigation, formal analysis, writing – original draft, validation. **Jens Hauslage:** investigation, writing – review and editing, validation.

Acknowledgements

Our heartfelt gratitude goes out to the MAPHEUS team at the Institute of Frontier Materials on Earth and in Space, German Aerospace Centre (DLR), Cologne, for allowing us to take part in the sounding rocket campaigns. We also want to thank the DLR Mobile Rocket Base (MORABA) and the Swedish Space Corporation (SSC) for their invaluable support during the campaigns. Our heartfelt appreciation is also given to the Ph.D. scholarship that is supported by the Joint Program of the Nottingham-Adelaide Alliance, provided by Adelaide University and the gracious support by ARC Centre of Excellence "Plants for Space" (P4S) with the grant number CE230100015.

Open access publishing facilitated by Adelaide University, as part of the Wiley - Adelaide University agreement via the Council of Australasian University Librarians

Funding

The MAPHEUS project is financed by the German Aerospace Centre.

Conflicts of Interest

The authors declare no conflicts of interest.

Data Availability Statement

The data that support the findings of this study are available from the corresponding author upon reasonable request.

References

1. M. Ikegame, A. Hattori, M. J. Tabata, et al., "Melatonin Is a Potential Drug for the Prevention of Bone Loss During Space Flight," *Journal of Pineal Research* 67, no. 3 (2019): 12594, https://doi.org/10.1111/jpi.12594.

2. J. Guo, S. Chen, X. Xu, et al., "Impacts of Microgravity on Circadian Rhythms and Regulatory Mechanisms," *Space: Science & Technology* 5 (2025): 0251, https://doi.org/10.34133/space.0251.

3. K. Barchetti, A. Derobertmasure, P. Boutouyrie, and P. Sestili, "Redefining Space Pharmacology: Bridging Knowledge Gaps in Drug Efficacy and Safety for Deep Space Missions," *Frontiers in Space Technologies* 5 (2024): 1456614, https://doi.org/10.3389/frspt.2024.1456614.

4. D. Russo, T. Bandiera, M. Monici, et al., "Physiological Adaptations Affecting Drug Pharmacokinetics in Space: What Do We Really Know? A Critical Review of the Literature," *British Journal of Pharmacology* 179, no. 11 (2022): 2538–2557, https://doi.org/10.1111/bph.15822.

5. J. Kast, Y. Yu, C. N. Seubert, V. E. Wotring, and H. Derendorf, "Drugs in Space: Pharmacokinetics and Pharmacodynamics in Astronauts," *European Journal of Pharmaceutical Sciences* 109S (2017): S2–S8, https://doi.org/10.1016/j.ejps.2017.05.025.

6. J. F. Reichard, S. E. Phelps, K. R. Lehnhardt, M. Young, and B. D. Easter, "The Effect of Long-term Spaceflight on Drug Potency and the Risk of Medication Failure," *npj Microgravity* 9 (2023): 35, https://doi.org/10.1038/s41526-023-00271-6.

7. Á. Simon, A. Smarandache, V. Iancu, and M. L. Pascu, "Stability of Antimicrobial Drug Molecules in Different Gravitational and Radiation Conditions in View of Applications During Outer Space Missions," *Molecules* 26, no. 8 (2021): 2221, https://doi.org/10.3390/molecules26082221.

8. V. R. Daniels, T. M. Bayuse, R. K. M. McGuire, E. L. Antonsen, and L. Putcha, "Radiation impact on pharmaceutical stability: Retrospective data review," *NASA Human Research Program Investigators' Workshop*, (NASA Johnson Space Center, 2017), Technical Report No. 09940.

9. D. Dantuma, R. Elmaddawi, Y. Pathak, et al., "Impact of Simulated Microgravity on Nanoemulsion Stability—a Preliminary Research," *American Journal of Medical and Biological Research* 3, no. 4 (2015): 102–106, https://doi.org/10.12691/ajmbr-3-4-4.

10. I. Seoane-Viaño, J. J. Ong, A. W. Basit, and A. Goyanes, "To Infinity and Beyond: Strategies for Fabricating Medicines in Outer Space," *International Journal of Pharmaceutics: X* 4 (2022): 100121, https://doi.org/10.1016/j.ijpx.2022.100121.

11. Y. Liu, X. Cao, Q. Zhou, et al., "Mechanisms and Countermeasures for Muscle Atrophy in Microgravity," *Cells* 13, no. 24 (2024): 2120, https://doi.org/10.3390/cells13242120.

12. S. Genah, M. Monici, and L. Morbidelli, "The Effect of Space Travel on Bone Metabolism: Considerations on Today's Major Challenges and Advances in Pharmacology," *International Journal of Molecular Sciences* 22, no. 9 (2021): 4585, https://doi.org/10.3390/ijms22094585.

13. B. E. Crucian, A. Choukèr, R. J. Simpson, et al., "Immune System Dysregulation During Spaceflight: Potential Countermeasures for Deep Space Exploration Missions," *Frontiers in Immunology* 9 (2018): 1437, https://doi.org/10.3389/fimmu.2018.01437.

14. F. P. M. Kohn and J. Hauslage, "The Gravity Dependence of Pharmacodynamics: The Integration of Lidocaine Into Membranes in Microgravity," *npj Microgravity* 5 (2019): 5, https://doi.org/10.1038/s41526-019-0060-5.

15. J. P. Vandenbrink and J. Z. Kiss, "Space, the Final Frontier: A Critical Review of Recent Experiments Performed in Microgravity," *Plant Science* 243 (2016): 115–119, https://doi.org/10.1016/j.plantsci.2015.11.004.

16. F. Ferranti, M. Del Bianco, and C. Pacelli, "Advantages and Limitations of Current Microgravity Platforms for Space Biology Research," *Applied Sciences* 11, no. 1 (2021): 68, https://doi.org/10.3390/app11010068.

17. A. J. Mortimer, "Use of Sounding Rockets in the Study of Microgravity Cell biology," in *Workshop on Microgravity Experimentation in Aircraft and Rockets*, NTIS Accession No. N8917036 (National Research Council of Canada/NASA Foreign Exchange Program, 1988), 95–97, https://ntrl.ntis.gov/NTRL/dashboard/searchResults/titleDetail/N8917036.xhtml?utm.

18. S. Kopp, M. Krüger, S. Feldmann, et al., "Thyroid Cancer Cells in Space During the TEXUS-53 Sounding Rocket Mission—The THYROID Project," *Scientific Reports* 8 (2018): 10355, https://doi.org/10.1038/s41598-018-28695-1.

19. Q. D. Tran, N. Spooner, S. Geoghegan, et al., "Cosmic-Ray Radiation Effects on Ibuprofen Tablet Formulation inside and outside of the International Space Station," *Advanced Healthcare Materials* 14, no. 4 (2025): 2402361, https://doi.org/10.1002/adhm.202402361.

20. A. N. Zaid, " a Comprehensive Review on Pharmaceutical Film Coating: Past, Present, and Future ," *Drug Design, Development and Therapy* 14 (2020): 4613–4623, https://doi.org/10.2147/DDDT.S277439.

21. K.-S. Seo, R. Bajracharya, S. H. Lee, and H.-K. Han, "Pharmaceutical Application of Tablet Film Coating," *Pharmaceutics* 12, no. 9 (2020): 853, https://doi.org/10.3390/pharmaceutics12090853.

22. M. Adebowale, N. V. D. Long, P. M. Williams, and V. Hessel, "Microfluidic Engineering of Chitosan-Coated Nanoemulsions for Controlled Release and Stability in Space Pharmaceutics," *Advanced Materials Technologies* 11, no. 12 (2026): 02201, https://doi.org/10.1002/admt.202502201.

23. N. Mishra, N. Kaushik, P. K. Sharma, and M. A. Alam, "Nano Emulsion Drug Delivery System: A Review," *Current Nanomedicine* 13, no. 1 (2023): 2–16, https://doi.org/10.2174/2468187313666230213121011.

24. Z. Rahiminezhad, S. Esteghlal, M. Hadian, G. R. Mesbahi, M. Golmakani, and S. M. H. Hosseini, "Effects of Nanoemulsions′ droplet Size and Natural Antioxidants′ hydrophilicity on Oxidative Stability and Mechanical Properties of Alginate Beads Filled With Linseed Oil Nanoemulsion," *Foods* 15, no. 3 (2026): 515, https://doi.org/10.3390/foods15030515.

25. S. Grijalvo and C. Rodriguez-Abreu, "Polymer Nanoparticles From Low-energy Nanoemulsions for Biomedical Applications," *Beilstein Journal of Nanotechnology* 14 (2023): 339–350, https://doi.org/10.3762/bjnano.14.29.

26. M. Bendersky, M. M. Santore, and J. M. Davis, "Statistically-based DLVO Approach to the Dynamic Interaction of Colloidal Microparticles With Topographically and Chemically Heterogeneous Collectors," *Journal of Colloid and Interface Science* 449 (2015): 443–451, https://doi.org/10.1016/j.jcis.2015.02.031.

27. A. Gupta, H. B. Eral, T. A. Hatton, and P. S. Doyle, "Nanoemulsions: Formation, Properties and Applications," *Soft Matter* 12, no. 11 (2016): 2826–2841, https://doi.org/10.1039/C5SM02958A.

28. S. Tamilvanan, B. A. Kumar, S. R. Senthilkumar, R. Baskar, and T. R. Sekharan, "Stability Assessment of Injectable Castor Oil-Based Nano-sized Emulsion Containing Cationic Droplets Stabilized by Poloxamer–Chitosan Emulsifier Films," *Aaps Pharmscitech [Electronic Resource]* 11, no. 2 (2010): 904–909, https://doi.org/10.1208/s12249-010-9455-3.

29. L. Espinosa-Sandoval, C. Ochoa-Martínez, A. Ayala-Aponte, L. Pastrana, C. Gonçalves, and M. A. Cerqueira, "Polysaccharide-based Multilayer Nano-emulsions Loaded With Oregano Oil: Production, Characterization, and in Vitro Digestion Assessment," *Nanomaterials* 11, no. 4 (2021): 878, https://doi.org/10.3390/nano11040878.

30. C. Diedrich, I. C. Zittlau, N. M. Khalil, et al., "Optimized Chitosan-based Nanoemulsion Improves Luteolin Release," *Pharmaceutics* 15, no. 6 (2023): 1592, https://doi.org/10.3390/pharmaceutics15061592.

31. M. Danaei, M. Dehghankhold, S. Ataei, et al., "Impact of Particle Size and Polydispersity Index on the Clinical Applications of Lipidic Nanocarrier Systems," *Pharmaceutics* 10, no. 2 (2018): 57, https://doi.org/10.3390/pharmaceutics10020057.

32. N. Aibani, R. Rai, P. Patel, G. Cuddihy, and E. K. Wasan, "Chitosan Nanoparticles at the Biological Interface: Implications for Drug Delivery," *Pharmaceutics* 13, no. 10 (2021): 1686, https://doi.org/10.3390/pharmaceutics13101686.

33. eds. M. Madi and O. Sokolova, *Space Debris Peril: Pathways to Opportunities*, 1st edn (CRC Press, 2020), https://doi.org/10.1201/9781003033899.

34. A. Datta, T. Kibria, and N. A. Tanisha, "Thermal Management for Lunar Rovers: Addressing Extreme Temperature Challenges," (Bangladesh University of Engineering and Technology, 2024), unpublished technical manuscript, https://doi.org/10.13140/RG.2.2.26726.48966.

35. J. Wang, "Why Do Spacecraft Always Experience a Black-out Area That Disrupts Communications When They Return to Earth?," in *ScienceOpen Preprints, Version 3* (2024), https://doi.org/10.14293/PR2199.000242.v3.

36. J. Park, S. Choi, and H. M. Jung, "Measurement and Analysis of Vibration Levels for Truck Transport Environment in Korea," *Applied Sciences* 10, no. 19 (2020): 6754, https://doi.org/10.3390/app10196754.

37. T. Trost, "Mechanical Stresses on Products During Air Cargo Transportation," *Packaging Technology and Science* 1, no. 3 (1988): 137–155, https://doi.org/10.1002/pts.2770010305.

38. R. W. Stanfield, "Sounding Rocket Flight Vibration gRMS/Re Ratio," *Journal of Spacecraft and Rockets* 63, no. 2 (2026): 511–522, https://doi.org/10.2514/1.A36444.

39. S. N. Jamthe, "How Much G-force Will You Experience in a SpaceX Falcon-9 Launch?," https://sjamthe.github.io/spacex-launch-analysis/, 13 April 2026 *GitHub Pages*, viewed.

40. J. Ding, H. Zhao, J. Wang, Y. Sun, and Z. Chen, "Numerical and Experimental Investigation on the Shock Mitigation of Satellite-rocket Separation," *Aerospace Science and Technology* 96 (2020): 105538, https://doi.org/10.1016/j.ast.2019.105538.

41. V. Rouillard and M. Sek, "Creating Transport Vibration Simulation Profiles From Vehicle and Road Characteristics," *Packaging Technology and Science* 26, no. 2 (2013): 82–95, https://doi.org/10.1002/pts.1967.

42. L. Iacovissi, N. Lu, and R. C. Williamson, "Corruptions of Supervised Learning Problems: Typology and Mitigations," *Journal of Machine Learning Research* 27, no. 72 (2026): 1–73.

43. C.-D. Hillenbrand, S. J. Crowhurst, M. Williams, et al., "New Insights From Multi-proxy Data From the West Antarctic Continental Rise: Implications for Dating and Interpreting Late Quaternary Palaeoenvironmental Records," *Quaternary Science Reviews* 257 (2021): 106842, https://doi.org/10.1016/j.quascirev.2021.106842.

44. M. Goyal and Q. H. Mahmoud, "A Systematic Review of Synthetic Data Generation Techniques Using Generative AI," *Electronics* 13, no. 17 (2024): 3509, https://doi.org/10.3390/electronics13173509.

45. P. Kokol, M. Kokol, and S. Zagoranski, "Machine Learning on Small Size Samples: A Synthetic Knowledge Synthesis," *Science Progress* 105, no. 1 (2022): 00368504211029777, https://doi.org/10.1177/00368504211029777.

46. W. H. Press, S. A. Teukolsky, W. T. Vetterling, and B. P. Flannery, *Numerical Recipes in C: The Art of Scientific Computing*, 2nd edn (Cambridge University Press, 1992).

47. S. Schmidt, M. N. Adebowale, E. V. Rebrov, et al., "Evaluating the Impact of Simulated Microgravity of a Random Positioning Machine on the Stability of Emulsions Applying Scaling Analysis via Dimensionless Numbers," *Soft Matter* 21 (2025): 8300–8322, https://doi.org/10.1039/D5SM00436E.

Supporting Information

Additional supporting information can be found online in the Supporting Information section.

Supporting File: adhm71521-sup-0001-SuppMat.docx.